RSC Advances

RSC Publishing

PAPER

View Article Online
View Journal | View Issue

Fractal porosity in metals synthesized by a simple combustion reaction†

Cite this: *RSC Advances*, 2013, **3**, 2351

Pedro Gómez-Romero,*[ab] Julio Fraile[c] and Belen Ballesteros[a]

Received 8th October 2012,
Accepted 5th December 2012

DOI: 10.1039/c2ra22441k

www.rsc.org/advances

A simple modification of a combustion method has been used for the production of ultraporous metals in air. Nitrates of different metallic elements were reacted with glycine as a reducing fuel. The glycine to nitrate ratio can be simply used to control the formation of oxides or, in the case of fuel-rich mixtures, the formation of metals such as Ni, Co, Cu or Ag. Furthermore, the metallic monoliths obtained present a remarkable porosity of fractal nature (from macro to nano scales) with pores ranging from many microns down to at least 5 nm. This exceedingly simple approach shows the way for the design and synthesis of complex porous microstructures of metals for the wide variety of applications where interface optimization is crucial.

Introduction

One of the greatest challenges facing materials science for the coming decades is the management of complexity in multiple length scales (macro, meso, micro). But this ever-growing complexity should not be accompanied by a matching level of intricacy in the fabrication processes. In recent decades a wealth of work has been devoted for instance to the control of macro- and meso-porosity through the use of pore-formers and surfactant-templated micelles, respectively.[1] Different tools for different dimensions. And when the desired porosity reaches the micro domain, still different molecular approaches need to be used. But in order to keep advancing the field of complexity, it will be necessary to use simple preparation methods and engineering techniques. In the case of porous materials for instance, the goal would be to induce hierarchically structured porosity without hierarchically varied tools. Furthermore, even better than hierarchical structures would be to get a continuous porosity going from the macro to the nanoworld. The reason lies in the wealth of applications which could benefit from an improved integral surface engineering which would include micro (nano-) meso and macro surfaces. Applications such as ultraporous metallic materials are of high relevance due to their technological applications in catalysis or electrocatalysis[2], sensing[3], biomedical engineering[4,5] or artificial muscles.[3,6] Methods to prepare them involve multi-step synthesis techniques like selective leaching or dealloying,[2,4,5,7–10] application of sacrificial templates[11–13] or the combination of combustion and chemical techniques.[14] The surface area of these materials depends on the preparation conditions and can vary between 0.5 $m^2 g^{-1}$[13] up to 20–300 $m^2 g^{-1}$.[15] Other relevant strategies for the synthesis of porous metals reported in literature include displacement of porous silicon,[16,17] hydrothermal synthesis with fatty acid templates,[18] sol–gel fabrication of hollow bimetallic microfibers,[19] or even the use of diatomites as support for catalytic bimetallic alloys.[20]

Some of these applications are truly limited by a lack of understanding and control of surface and porosity, while they require optimization and maximization of complex interfaces (solid–gas solid–electrolyte) even triple interfaces (solid–electrolyte–gas) in the case of fuel cells for instance.

As part of our ongoing research on the development of materials for fuel cells we have systematically worked on the synthesis of NiO, Ni and Ni-based cermets and have found, and report here, surprising results which are more far-reaching and with possible applications beyond fuel cells. We report a fast, simple, reproducible, single-step method to obtain metallic nickel sponges with fractal porosity (from microns to nanometre size). The synthesis is based on the well-known glycine–nitrate combustion technique where a metal nitrate is used as oxidizing agent and glycine as the fuel. This method has been frequently used to prepare high surface area metal oxide materials,[21] but no pure-metallic structures had been obtained just through this technique when we carried out this work. Very recently (note added in proof by suggestion of a referee) Deraz reported a similar synthesis of Ni in a narrow synthetic conditions range.[22,23] Remarkably and surprisingly, the simple control of the amount of glycine provides the means to obtain not only oxides but also even pure metals as it will be shown.

[a]*Centro de Investigación en Nanociencia y Nanotecnología, CIN2 (CSIC-ICN), Bellaterra, Barcelona, Spain, E-08193. E-mail: pedro.gomez@cin2.es; Fax: +34 93 5868020; Tel: +34 93 5868010*
[b]*MATGAS Research Center, Campus UAB, Bellaterra, Barcelona, Spain, E-08193*
[c]*ICMAB (CSIC), Campus UAB, Bellaterra, Barcelona, Spain, E-08193*
† Electronic supplementary information (ESI) available: BET adsorption isotherms and BJH pore analyses for each sample. See DOI: 10.1039/c2ra22441k

We used different glycine-to-nitrate ratios and found that a fuel-rich stoichiometry, that is, an excess of the reducing agent, was the simple key to produce monoliths of nickel in its metallic state. These Ni sponges were thus produced in a single step reaction open to the air, challenging conventional wisdom for the need of reducing atmospheres (normally hydrogen) in order to reach the reduced metal state.[13] Furthermore, we expanded our work to show the generality of the method to other metals, as it will be shown below.

Experimental

Hydrated metal nitrates and glycine from Aldrich were used as received. In a typical reaction, $Ni(NO_3)_2 \cdot 6H_2O$ and glycine (mole ratio 1 : 2) were dissolved in the minimum amount of deionized water with stirring, The solution was heated in a 2 litre beaker on a hot plate until a viscous green gel was formed and eventually dried out. The heating was maintained until ignition of the mixture took place leading to a spontaneous combustion reaction proceeding smoothly at *ca.* 250 °C (heating plate) with an orange flame spreading in a few seconds from a single ignition point until the whole mixture had reacted leaving a porous ash-like residue of metallic nickel.

SEM analyses were performed in a Stereoscan S-360 equipped with EDX, INCA Energy 200 Oxford Instruments with Be detector. The equipment was fixed for high resolution images at 6 mm distance, 10 kV and 50 pA. The samples were mounted on aluminium stubs. The materials were analyzed after being sputter-coated with gold. In cases where the material presented good metallic properties (like metallic nickel) no coating was required. High resolution images were obtained with a Hitachi H-4 100 FE SEM.

X-Ray diffraction analyses were performed using a Rigaku, Rotaflex Ru-200 B with Cu-Kα (λ = 1.5418), from 5 to 80° and step intervals of 0.02°. Elemental analysis was performed in a Carlo Erba CHN EA 1108 equipment at maximum temperature of 1800 °C. Pore size analyses were carried out in a 'Pore Master' Porosimeter from Quantachrome Instruments which analyzes pore volume of pores with diameter between 0.0070–400 microns by intrusion between 5% to 95% of 0.5 cc of Hg. BET analyses were carried out in a Micrometrics ASAP 2000, the samples were degased in vacuum for 14 h before testing.

Results and discussion

The synthesis was carried out as described above and led to an ash-looking material. Scanning electron microscopy (SEM) images of that material (Fig. 1a) show the macroscopic spongy morphology of the millimetre-sized nickel monoliths obtained. As we analyse the same sample under higher and higher magnifications we detect a recurrent pattern, a distribution of pores with different sizes. Thus, in going from Fig. 1b through e, we can see in every case how large pores are surrounded by smaller ones, the latter coming out in turn as large pores in the next magnification scale.

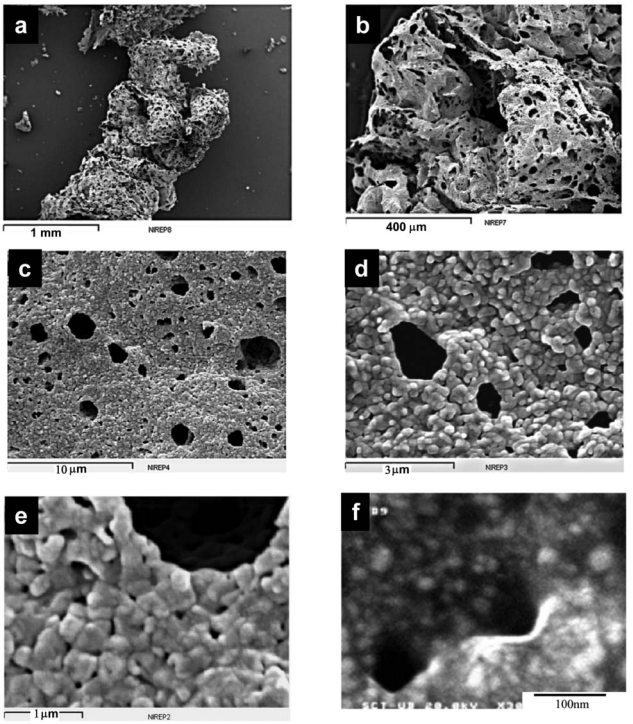

Fig. 1 SEM images of metallic nickel showing a microstructure with porosity apparent at different length scales. In the higher magnification photo (f) (recorded with Field Emission SEM) it becomes apparent that the structure is made of nickel nanoparticles much smaller than 100 nm sintered together but retaining an open porosity.

This fractal nature of porosity in our metallic samples extends through a remarkable range spanning from millimetres to microns to nanometres. In order to determine the nanoporosity in a more precise way that Fig. 1e could provide, we recorded additional high-resolution images with a field emission SEM microscope. Fig. 1f shows both the nanoparticulate nature of the solid sample as well as the minimal pore size we were able to detect with this technique corresponding to pores of *ca.* 50 nm. The morphology of the whole nickel monoliths encompass metallic nickel nanoparticles of sizes between 15–40 nm sintered together (Fig. 1f) at the high local temperatures reached during synthesis, generating nickel aggregates of about 200–400 nm (Fig. 1e). Porosity is shaped by the combustion gases that break out during the reaction precluding the 200–400 nm nickel micro particles from sintering and leading to a hierarchical pore distribution.

The isolation of pure nickel was confirmed by X-ray powder diffraction (Fig. 2a). Three major peaks with d spacings 2.03, 1.76 and 1.24 Å can be indexed as fcc Ni, a phase stable at high temperature, in good agreement with the high local temperatures characteristic of the method. Marginally visible peaks at 2.40, 2.08, 2.47 Å (corresponding to NiO) and at 2.3, 2.15, 1.57 and 1.33 (from Ni_3N) can also be detected. NiO has been proposed as intermediate species produced in the course of

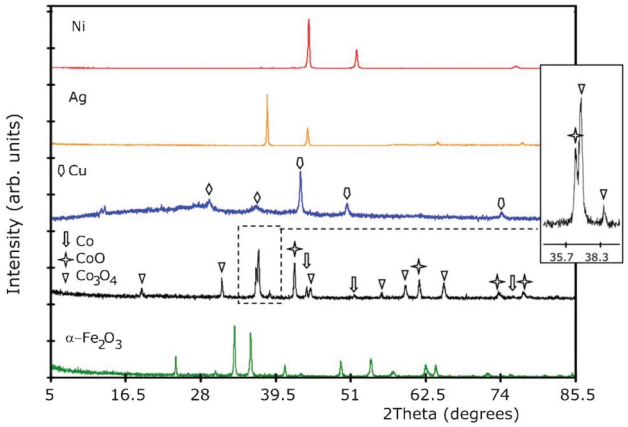

Fig. 2 X-Ray diffraction patterns of the products obtained for different metal ions through the glycine combustion method in air.

this type of reactions.[22,23] However, our final sample is essentially NiO-free. Elemental analyses showed 0.39% N and 0.13% C. Both impurities are close to the detection limit confirming an essentially pure metallic sample.

In order to test the generality of the method, the synthesis of other materials was also carried out. The same procedure leading to essentially pure Ni metal led to metals such as Cu and Ag, or to pure oxides like Fe_2O_3, or Al_2O_3. X-Ray analyses showed the formation of Ag, Cu and Ni in the metallic state and pure γ-Fe_2O_3 in its maghemite, form (Fig. 2). Fittingly, cobalt represents an intermediate case for which mixtures of the metal and its oxides where obtained (Fig. 2). In all cases the syntheses proceeded in the same single-step conditions and followed a smooth and non-violent path. Only in the case of copper the combustion reaction was brisk and took place with spewing out part of the product, leaving a plate-like morphology settled on the bottom of the beaker and well-defined spherical particles deposited on the beaker walls. Fig. 3 shows the porous nature of all these materials closely resembling that of Ni described in more detail in Fig. 1.

In order to ascertain the fractal hierarchical nature of porosity we also used BET gas absorption (Brunauer–Emmet–Teller) and mercury porosimetry analyses. Preliminary measurements for our original Ni foams revealed a wide pore-diameter distribution with the presence of pore diameters as small as *ca.* 5 nm, a surface area of 4.2 m^2g^{-1} and an average pore fraction of 56% of the sample.

Fig. 4 plots pore volume as a function of pore diameter for the whole series of materials studied. In all cases there is a wide range of pore diameters ranging from 2–5 nm up to 100 nm with a minimum for pore diameters of *ca.* 10 nm. Thus, fractal porosity characterizes all the materials studied.

A trend of pore volume and surface area as a function of the material prepared is also clear from Fig. 4.

Thus, pore volume increase according to Fe > Co > Ni > Ag. The same trend is also detected for surface area: iron oxide shows a surface area of 17 $m^2\ g^{-1}$, followed by cobalt/cobalt oxides, 6.32 $m^2\ g^{-1}$, metallic nickel 4.21 $m^2\ g^{-1}$ and finally

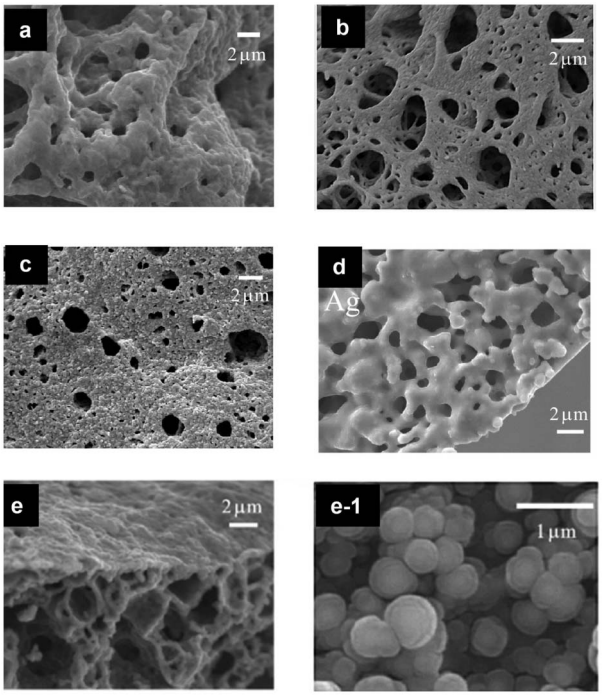

Fig. 3 SEM images of the products resulting from the nitrate–glycine reaction starting from iron(III) nitrate (a), cobalt(II) (b), Ni(II) (c), Ag(I) (d) and Cu(II) (e). The latter includes two photographs corresponding to the plates (e) and spherical particles on the walls (e1) (see text).

metallic silver with 1.18 $m^2\ g^{-1}$. The exception for both, pore volume and surface area, was observed for copper with the highest surface area of all materials (77 $m^2\ g^{-1}$) and wild pore size distribution, the latter possibly due to the dual morphology observed for the final product resulting from the vigorous reaction behaviour. In Fig. 4 this results in data for Cu featuring an order of magnitude larger pore volume than the other materials.

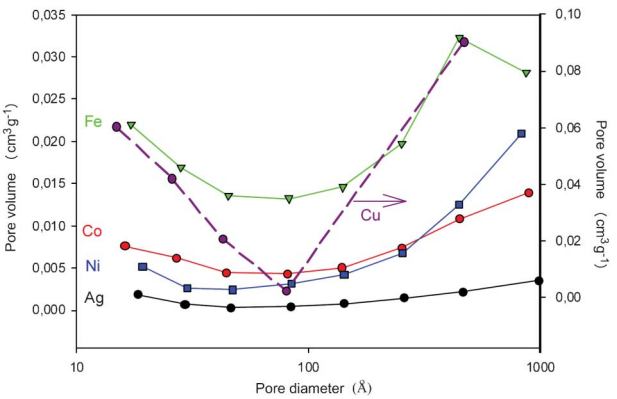

Fig. 4 Pore diameter *vs.* pore volume measured by BET found in different samples obtained by the glycine–nitrate combustion method. All data except Cu are referred to the left y axis. The vertical axis on the right is just for Cu. The anomalous values found for Cu must be related to the fact that its synthesis was the only one taking place in an abrupt way (see text).

Conclusions

We have demonstrated a simple and effective modification of the glycine–nitrate combustion synthesis to obtain metals or metal oxide materials with fractal porosity. The novelty of our work is double. First we are able to obtain metals (and not just noble metals such as Ag) very easily in air. Secondly, the materials prepared present a remarkable hierarchically-graded microstructure with effective fractal porosity. The materials are prepared in a single-step reaction without the need of further treatments. The resulting structures are formed by the partial sintering of metal or metal oxide particles between 150–500 nm in size. The voids left behind produce a structure with 56% porosity and more than about 4 $m^2 g^{-1}$ of surface area for the case of metallic nickel. The hierarchical pore size range from microns to nanometers making these materials suitable for a wide variety of applications for which interfaces should be optimized. Furthermore, the method could also be explored for the design of not only pure metals or oxides but also of ceramic-metal nanocomposite materials.

Acknowledgements

Partial funding from the Spanish Ministry MAT2011-28931 is acknowledged. We thank MLC for the preparation of some samples.

Notes and references

1 M. Kruk, *Acc. Chem. Res.*, 2012, **45**(10), 1678–1687.
2 A. Katagiri and M. Nakata, *J. Electrochem. Soc.*, 2003, **150**, C585–C590.
3 J. Weissmüller, *et al.*, *Science*, 2003, **300**, 312–315.
4 D. V. Pugh, A. Dursun and S. G. Corcoran, *J. Mater. Res.*, 2003, **18**, 216–221.
5 A. Dursun, D. V. Pugh and S. G. Corcoran, *J. Electrochem. Soc.*, 2003, **150**, B355–B360.
6 R. H. Baughman, *Science*, 2003, **300**, 268–269.
7 J. Erlebacher, *et al.*, *Nature*, 2001, **410**, 450–453.
8 M. Rajamati, *et al.*, *J. Mater. Chem.*, 2001, **11**, 2489–2492.
9 M. Stratmann and M. Rohwerder, *Nature*, 2001, **410**, 420–422.
10 Y. Ding and J. Erlebacher, *J. Am. Chem. Soc.*, 2003, **125**, 7772–7773.
11 K. M. Kulinowski, *et al.*, *Adv. Mater.*, 2000, **12**, 833–838.
12 O. D. Velev and E. W. Kaler, *Adv. Mater.*, 2000, **12**, 531–534.
13 D. Walsh, *et al.*, *Nat. Mater.*, 2003, **2**, 386–390.
14 M. Panda, M. Rajamathi and R. Seshadri, *Chem. Mater.*, 2002, **14**, 4762–4767.
15 S. Raush and H. Wendt, *J. Electrochem. Soc.*, 1996, **143**, 2852–2862.
16 M. Hayase, T. Matsuzaka and J. G. Alves Brito-Neto, *ECS Trans.*, 2008, **16**, 231–235.
17 H. Bandarenka, S. Redko, A. Smirnov, A. Panarin, S. Terekhov, P. Nenzi, M. Balucani and V. Bondarenko, *Nanoscale Res. Lett.*, 2012, **7**, 477.
18 A. K. Patra, A. Dutta and A. Bhaumik, *Catal. Commun.*, 2010, **11**, 651–655.
19 X. Shen, L. Guo, M. Liu, F. Song and Y. Zhu, *Mater. Lett.*, 2011, **65**, 2841–2843.
20 Y. Chen, M. Xiao, S. Wang, D. Han, Y. Lu and Y. Meng, *J. Nanomater.*, 2012, **2012**, 610410.
21 R. D. Purohit, B. P. Sharma, K. T. Pillai and A. K. Tyagi, *Mater. Res. Bull.*, 2001, **36**, 2711–2721.
22 N. M. Deraz, *Curr. Appl. Phys.*, 2012, **12**, 928–934.
23 N. M. Deraz, *Int. J. Electrochem. Sci.*, 2012, **7**, 4608–4616.

